

A Mesoporous Silica Nanosphere-Based Carrier System with Chemically Removable CdS Nanoparticle Caps for Stimuli-Responsive Controlled Release of Neurotransmitters and Drug Molecules

Cheng-Yu Lai,[†] Brian G. Trewyn,[†] Dusan M. Jeftinija,[‡] Ksenija Jeftinija,[‡] Shu Xu,[†] Srdija Jeftinija,[‡] and Victor S.-Y. Lin^{*†}

Contribution from the Department of Chemistry and Department of Biomedical Sciences, Iowa State University, Ames, Iowa 50011-3111

Received September 23, 2002; E-mail: vsylin@iastate.edu

Abstract: An MCM-41 type mesoporous silica nanosphere-based (MSN) controlled-release delivery system has been synthesized and characterized using surface-derivatized cadmium sulfide (CdS) nanocrystals as *chemically removable caps* to encapsulate several pharmaceutical drug molecules and neurotransmitters inside the organically functionalized MSN mesoporous framework. We studied the stimuli-responsive release profiles of vancomycin- and adenosine triphosphate (ATP)-loaded MSN delivery systems by using disulfide bond-reducing molecules, such as dithiothreitol (DTT) and mercaptoethanol (ME), as *release triggers*. The biocompatibility and delivery efficiency of the MSN system with neuroglial cells (astrocytes) in vitro were demonstrated. In contrast to many current delivery systems, the molecules of interest were encapsulated inside the porous framework of the MSN not by adsorption or sol–gel types of entrapment but by capping the openings of the mesoporous channels with size-defined CdS nanoparticles to physically block the drugs/neurotransmitters of certain sizes from leaching out. We envision that this new MSN system could play a significant role in developing new generations of site-selective, controlled-release delivery nanodevices.

Introduction

Several attractive features, such as stable mesoporous structures, large surface areas, tunable pore sizes and volumes, and well-defined surface properties of the organically functionalized MCM-type mesoporous silica materials¹ have made them ideal for hosting molecules of various sizes, shapes, and functionalities. Therefore, developing new mesoporous silica-based carrier systems for controlled-release delivery of drugs,² biocides, genes, or even proteins³ in vitro or in vivo is of keen interest.

Many important site-selective deliveries, e.g., deliveries of highly toxic antitumor drugs, such as Taxol, require “zero release” before reaching the targeted cells or tissues. However, the release of encapsulated compounds of many current drug

delivery systems typically takes place immediately upon dispersion of the drug/carrier composites in water.⁴ Also, the release mechanism of many biodegradable polymer-based drug delivery systems relies on the hydrolysis-induced erosion of the carrier structure.⁵ Such systems typically require the use of organic solvents⁶ for drug loading, which could sometimes trigger undesirable modifications of the structure or function or both of the encapsulated molecules, such as protein denaturation and aggregation.

Herein, we report the synthesis of a novel MCM-41 type mesoporous silica-based controlled-release delivery system that is stimuli-responsive and chemically inert to the matrix-entrapped compounds. The system consists of a 2-(propyldi-sulfanyl)ethylamine functionalized mesoporous silica nanosphere (MSN) material with an average particle size of 200.0 nm and an average pore diameter of 2.3 nm. As depicted in Figure 1, the mesopores of the MSN material were used as reservoirs to soak up aqueous solutions of various pharmaceutical drug molecules and neurotransmitters, such as vancomycin and adenosine triphosphate (ATP). The openings of the mesopores

* To whom correspondence should be addressed. Phone: (515) 294-3135.

[†] Department of Chemistry.

[‡] Department of Biomedical Sciences.

- (1) (a) Stein, A.; Melde, B. J.; Schroden, R. C. *Adv. Mater. (Weinheim, Ger.)* **2000**, *12*, 1403–1419. (b) Sayari, A.; Hamoudi, S. *Chem. Mater.* **2001**, *13*, 3151–3168 and references therein.
- (2) (a) Vallet-Regi, M.; Ramila, A.; del Real, R. P.; Perez-Pariente, J. *Chem. Mater.* **2001**, *13*, 308–311. (b) Munoz, B.; Ramila, A.; Perez-Pariente, J.; Diaz, I.; Vallet-Regi, M. *Chem. Mater.* **2003**, *15*, 500–503. (c) Ramila, A.; Munoz, B.; Perez-Pariente, J.; Vallet-Regi, M. *J. Sol.-Gel Sci. Technol.* **2003**, *26*, 1199–1202.
- (3) (a) Diaz, J. F.; Balkus, K. J., Jr. *J. Mol. Catal. B: Enzym.* **1996**, *2*, 115–126. (b) Han, Y.-J.; Stucky, G. D.; Butler, A. J. *Am. Chem. Soc.* **1999**, *121*, 9897–9898. (c) Kisler, J. M.; Dahler, A.; Stevens, G. W.; O'Connor, A. J. *Microporous Mesoporous Mater.* **2001**, *44–45*, 769–774. (d) Yiu, H. H. P.; Wright, P. A.; Botting, N. P. *Microporous Mesoporous Mater.* **2001**, *44–45*, 763–768. (e) Takahashi, H.; Li, B.; Sasaki, T.; Miyazaki, C.; Kajino, T.; Inagaki, S. *Microporous Mesoporous Mater.* **2001**, *44–45*, 755–762.

- (4) (a) Radin, S.; Ducheyne, P.; Kamplain, T.; Tan, B. H. *J. Biomed. Mater. Res.* **2001**, *57*, 313–320. (b) Aughenbaugh, W.; Radin, S.; Ducheyne, P. *J. Biomed. Mater. Res.* **2001**, *57*, 321–326. (c) Kortessuo, P.; Ahola, M.; Kangas, M.; Kangasniemi, I.; Yli-Urpo, A.; Kiesvaara, J. *Int. J. Pharm.* **2000**, *200*, 223–229.
- (5) (a) Uhrich, K. E.; Cannizzaro, S. M.; Langer, R. S.; Shakesheff, K. M. *Chem. Rev.* **1999**, *99*, 3181–3198. (b) Langer, R. *Acc. Chem. Res.* **1993**, *26*, 537–542 and references therein.
- (6) Li, Y.; Kissel, T. *J. Controlled Release* **1993**, *27*, 247–257 and references therein.

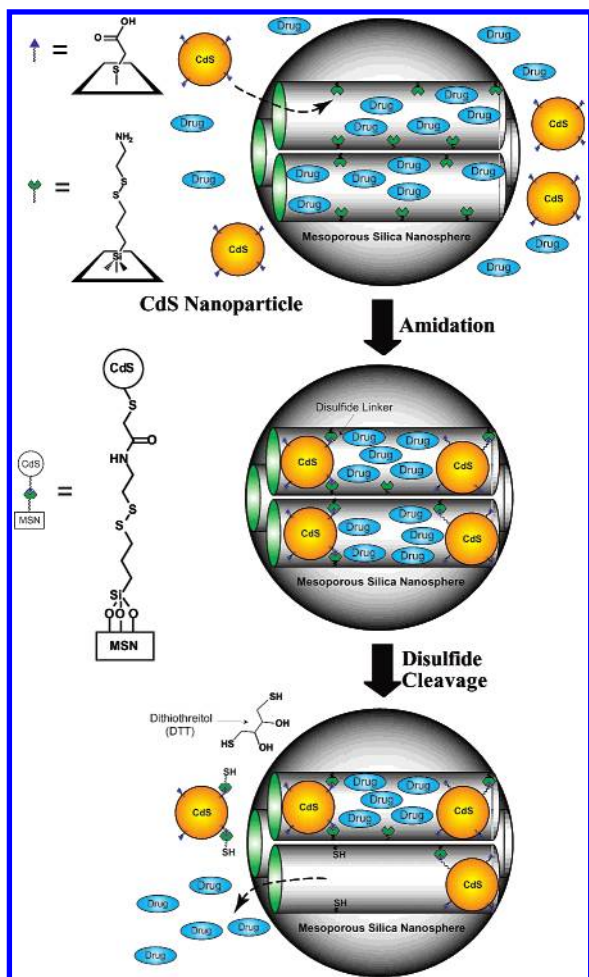


Figure 1. Schematic representation of the CdS nanoparticle-capped MSN-based drug/neurotransmitter delivery system. The controlled-release mechanism of the system is based on chemical reduction of the disulfide linkage between the CdS caps and the MSN hosts.

of the drug/neurotransmitter-loaded MSN material were then capped in situ by allowing the pore surface-bound 2-(propyldisulfanyl)ethylamine functional groups to covalently capture the water-soluble mercaptoacetic acid-derivatized cadmium sulfide (CdS) nanocrystals⁷ via a literature-reported amidation reaction.⁸ The resulting disulfide linkages between the MSNs and the CdS nanoparticles are *chemically labile* in nature and can be cleaved with various disulfide-reducing agents, such as dithiothreitol (DTT) and mercaptoethanol (ME). Hence, the release of the CdS nanoparticle caps from the drug/neurotransmitter-loaded MSNs can be regulated by introducing various amounts of *release triggers*. In this study, we investigated the stimuli-responsive release profiles, the biocompatibility with neuroglial cells (astrocytes) in vitro, and the delivery efficiency of vancomycin and adenosine triphosphate (ATP) encapsulated inside the CdS-capped MSN system.

Results and Discussion

To prepare the MSN material functionalized with a chemically labile linker that can covalently capture the CdS nanoparticles, we first synthesized a mercaptopropyl-derivatized mesoporous silica nanosphere material (thiol-MSN) via our recently reported

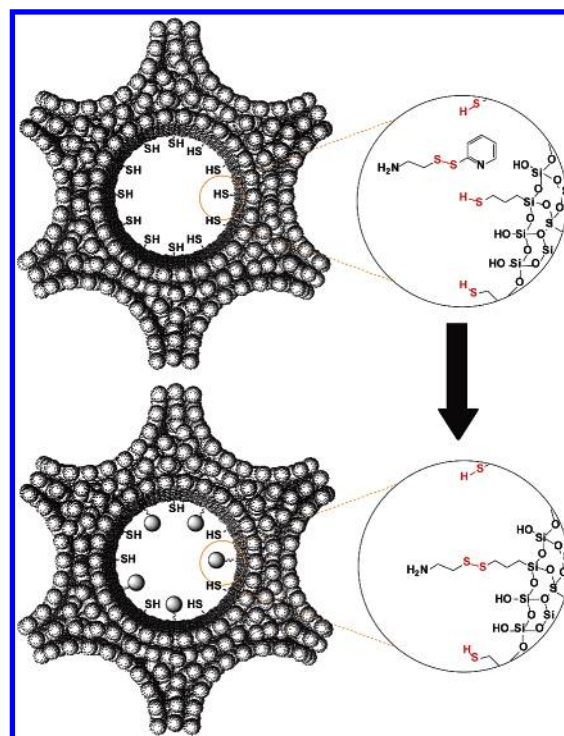


Figure 2. Synthesis of 2-(propyldisulfanyl)ethylamine functionalized mesoporous silica nanosphere (linker-MSN) material.

co-condensation method.⁹ As illustrated in Figure 2, the surfactant-removed thiol-MSN material was treated with a methanol solution of 2-(pyridyldisulfanyl)ethylamine, which was synthesized via a literature procedure,¹⁰ at room temperature for 24 h under vigorous stirring to yield the MSN material with 2-(propyldisulfanyl)ethylamine functionality (linker-MSN).

As depicted in Figure 3a, b, c, and e, the spherical particle shape and the MCM-41 type of hexagonally packed mesoporous structure of the linker-MSN material are confirmed by scanning and transmission electron microscopy (SEM and TEM, respectively). The N₂ adsorption/desorption isotherms of the material further revealed a BET isotherm typical of MCM-41 structure (type IV) with a surface area of 941.0 m²/g and a narrow BJH pore size distribution (average pore diameter = 2.3 nm).¹¹ The linker-MSN (100.0 mg) was used as a chemically inert host to soak up the aqueous solutions of vancomycin (3.0 μmol) and ATP (15.5 μmol).

To design a chemically removable cap, we synthesized a mercaptoacetic acid-coated, photoluminescent CdS nanocrystal material with an average particle diameter of 2.0 nm via a literature-reported procedure.⁷ As illustrated in Figure 1, the water-soluble CdS nanocrystals with mercaptoacetic acid groups were covalently captured and formed amide bonds by reacting with the mesopore surface-bound 2-(propyldisulfanyl)ethylamine linkers of the MSN/drug composite material in aqueous solutions. The resulting reaction suspensions were centrifuged, and the CdS-capped MSN/drug composite materials along with the

(7) Colvin, V. L.; Goldstein, A. N.; Alivisatos, A. P. *J. Am. Chem. Soc.* **1992**, *114*, 5221–5230.

(8) Chan, W. C.; Nie, S. *Science (Washington, D. C.)* **1998**, *281*, 2016–2018.

(9) (a) Lin, V. S.-Y.; Lai, C.-Y.; Huang, J.; Song, S.-A.; Xu, S. *J. Am. Chem. Soc.* **2001**, *123*, 11510–11511. (b) Lin, V. S.-Y.; Radu, D. R.; Han, M.-K.; Deng, W.; Kuroki, S.; Shanks, B. H.; Pruski, M. *J. Am. Chem. Soc.* **2002**, *124*, 9040–9041.

(10) Ebright, Y. W.; Chen, Y.; Kim, Y.; Ebright, R. H. *Bioconjugate Chem.* **1996**, *7*, 380–384.

(11) See Supporting Information for the BET isotherm, BJH pore size distribution, and solid-state ¹³C CP/MAS NMR spectra of both the linker-MSN and the CdS-capped MSN materials.

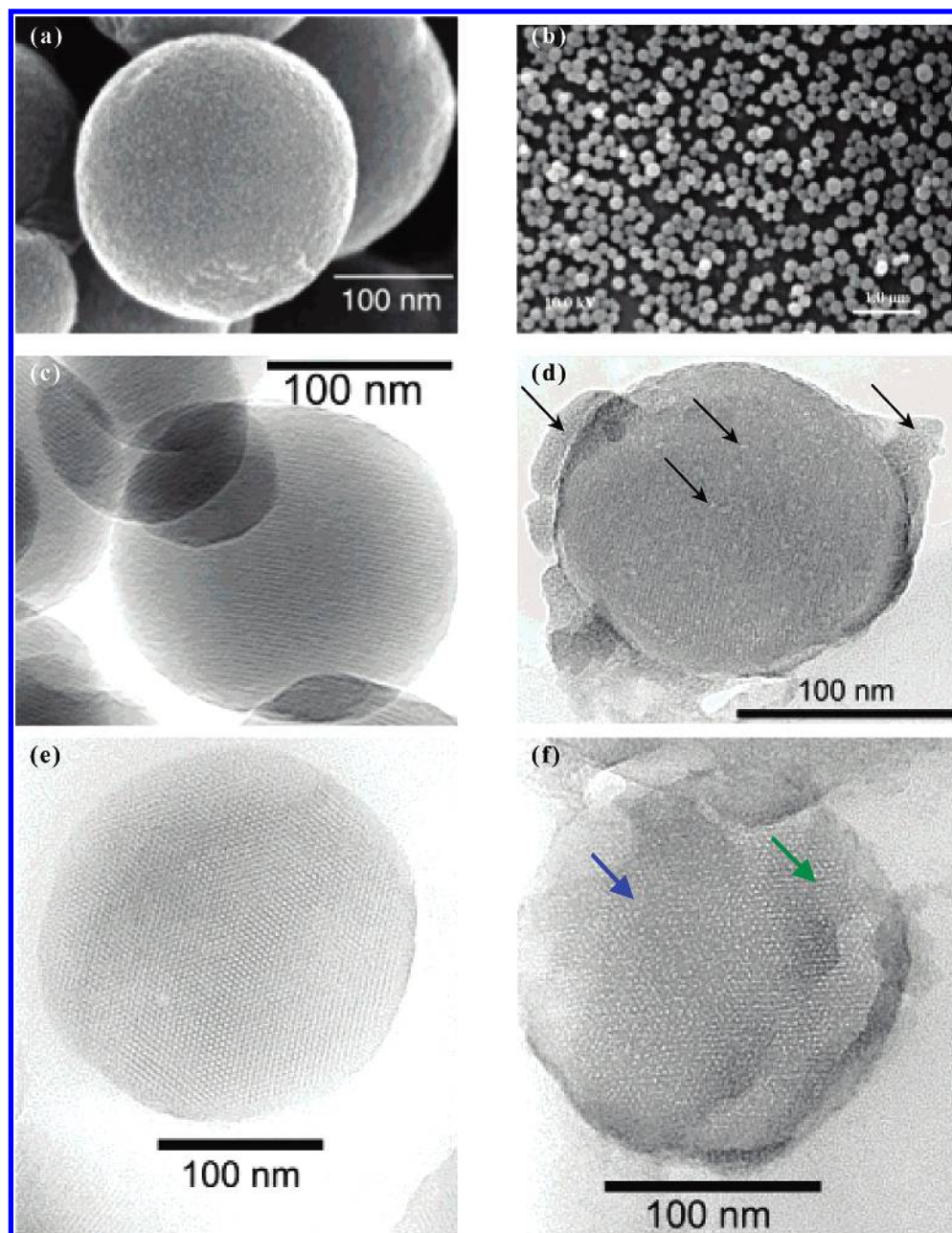


Figure 3. SEM (a and b) and TEM (300 kV) micrographs of the linker-MSN (c and e). The MCM-41 type of mesoporous channel structure of the nanospheres is visualized with the parallel stripes (c) and the hexagonally packed light dots (e) shown in the micrographs. The TEM micrographs (d and f) of the CdS-capped MSN clearly exhibit aggregations of CdS nanoparticles on the exterior surface of MSN material represented by dots in the areas indicated by black arrows in (d). A large area (left side of the MSN particle indicated by the blue arrow) displaying light dots packed in a disordered symmetry and an area (green arrow) where the mesopores are hexagonally arranged represent the CdS nanoparticle-capped and uncapped areas of MSN particle shown in (f), respectively. The TEM micrographs (d–f) were measured on ultramicrotomed samples with section thickness of 60–80 nm.

unreacted CdS nanoparticles were filtered. The concentrations of the free vancomycin and ATP molecules in the filtrate were then determined by HPLC. The calculated concentration decreases of solution vancomycin and ATP were attributed to the amounts of mesopore-encapsulated vancomycin (2.5 μmol) and ATP (4.7 μmol) per 100.0 mg of linker-MSN material. These numbers correspond to ca. 83.9 and 30.3 mol % loading efficiency, respectively.

The successful incorporation of CdS nanoparticles to the MSN matrix was confirmed by various spectroscopy methods.¹¹ As shown in Figure 4a, the covalent immobilization of the surface-functionalized CdS nanoparticles to the linker-MSN material reduced the intensity of the powder X-ray diffraction (XRD)

peaks. Such a reduction of scattering contrast between the pores and the framework of the MCM-41 materials due to the pore-filling effect has been reported previously in the literature.¹² Compared with the d_{100} value of the linker-MSN material, a small increase in that of CdS-capped MSN was observed. The increase of the d_{100} values may be attributed to the covalent linkage induced pore-filling effect between the CdS nanopar-

- (12) (a) Marler, B.; Oberhagemann, U.; Vortmann, S.; Gies, H. *Microporous Mater.* **1996**, *6*, 375–383. (b) Winkler, H.; Birkner, A.; Hagen, V.; Wolf, I.; Schmechel, R.; Von Seggern, H.; Fischer, R. A. *Adv. Mater. (Weinheim, Ger.)* **1999**, *11*, 1444–1448. (c) Zhang, W.-H.; Shi, J.-L.; Wang, L.-Z.; Yan, D.-S. *Chem. Mater.* **2000**, *12*, 1408–1413. (d) Zhang, W.-H.; Shi, J.-L.; Chen, H.-R.; Hua, Z.-L.; Yan, D.-S. *Chem. Mater.* **2001**, *13*, 648–654.

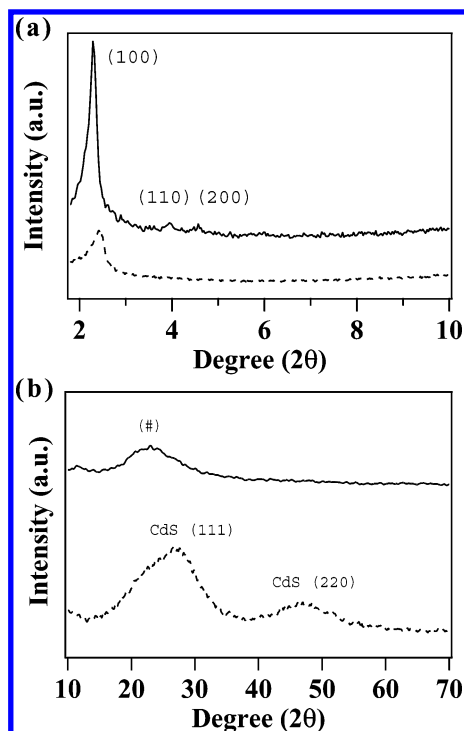


Figure 4. Low (a) and high (b) angle powder X-ray diffraction patterns (XRD) of the linker-MSN material before (solid line) and after (dashed line) the immobilization of CdS nanocrystals. (# is the diffuse peak of noncrystalline silica.)

ticles and the mesoporous silica matrix. Figure 4b showed the high-angle XRD diffraction patterns of the linker-MSN and the CdS-capped MSN materials within the 2θ range of 10° – 70° . In contrast to the low-intensity diffuse peak of noncrystalline silica observed in the linker-MSN material (Figure 4b), two additional peaks are detected in the CdS-capped MSN sample. As depicted in Figure 4b, these two peaks are attributed to the diffraction of (111) and (220) lattice planes of the CdS nanoparticles attached to the mesoporous silica.¹³ To further confirm that these CdS nanoparticle “caps” were indeed covalently linked to the mesopore surface-bound linker groups, the ^{13}C solid-state CP-MAS NMR spectra of both the CdS-capped MSN and the linker-MSN were carefully compared and the existence of the covalent linkage between the CdS and MSN materials was clearly observed as shown in the Supporting Information section.¹¹

TEM investigations of the CdS-capped MSN also provided direct evidence of the CdS distribution both on and in the organically functionalized MSN material. As shown in Figure 3d, where the mesopores (porous channels) are represented by the alternating black and white stripes, the CdS nanoparticles are clearly visible on the outside edge and inside the mesopores of the MSN depicted by the lighter areas (indicated by the arrowheads). As opposed to these features observed in the case of CdS-capped MSN, the TEM micrograph of the linker-MSN (Figure 3c) prior to the CdS “capping” showed smooth edges

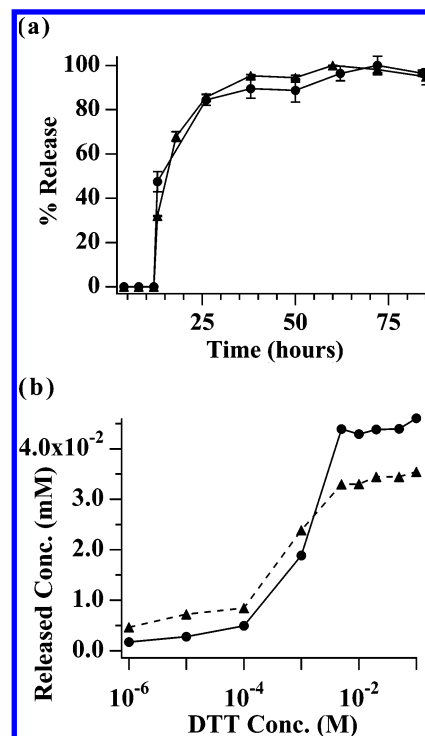


Figure 5. The DTT-induced release profiles of Vancomycin (—●—) and ATP (---▲---) from the CdS-capped MSN system: (a) % release over time. (b) The DTT concentration-dependent releases. Released analyte concentrations were measured with CdS-MSNs (2.3 mg) in pH 7.4 PBS buffers (0.8 mL) after 24 h of the DTT additions.

and nice contrasts between the mesoporous channels and the silica matrix. Furthermore, compared with the periodically well-organized hexagonal array of mesopores represented by the bright dots shown on the TEM micrograph of the linker-MSN orientated along the pore axis (Figure 3e), an additional layer of CdS nanoparticles on the outside of the MSN material and a large area of disordered hexagonal array of mesopores indicated by the arrows in Figure 3f were observed in the case of CdS-capped MSN material. In contrast to the “disordered” area, a small area with mesopores that are packed with a hexagonal symmetry was also noticed on the micrograph. These different areas could be attributed to the fact that most, but not all, mesopores are capped with the CdS nanoparticles.

As shown in Figure 5a, the CdS-capped MSN drug/neurotransmitter delivery system exhibited less than 1.0% of drug release in 10 mM PBS buffer solutions (pH 7.4) over a period of 12 h. The result suggested a good capping efficiency of the CdS nanoparticles for encapsulation of the vancomycin and ATP molecules against the undesired leaching problem. Addition of disulfide-reducing molecules, such as DTT and ME, to the aqueous suspension of CdS-capped MSNs triggered a rapid release of the mesopore-entrapped drug/neurotransmitter. Within 24 h, the release reached 85% of the total release seen in 3 days of vancomycin and ATP after the introduction of 18.5 mM DTT (Figure 5a). Interestingly, the rates of release of vancomycin and ATP showed similar diffusional kinetic profiles, indicating the lack of interaction between these released molecules and the mesoporous silica matrix. However, 53.8% (1.6 μmol) of the encapsulated vancomycin was released after 3 days of the DTT-induced uncapping of the mesopores, while only 28.2% (1.3 μmol) of the entrapped ATP molecules was able to diffuse away. Such a large difference between the portion

(13) (a) Kumar, A.; Mandale, A. B.; Sastry, M. *Langmuir* **2000**, *16*, 9299–9302. (b) Diaz, D.; Rivera, M.; Ni, T.; Rodriguez, J.-C.; Castillo-Blum, S.-E.; Nagesha, D.; Robles, J.; Alvarez-Fregoso, O.-J.; Kotov, N. A. *J. Phys. Chem. B* **1999**, *103*, 9854–9858. (c) Weller, H.; Schmidt, H. M.; Koch, U.; Fojtik, A.; Baral, S.; Henglein, A.; Kunath, W.; Weiss, K.; Dieman, E. *Chem. Phys. Lett.* **1986**, *124*, 557–560. (d) Yang, J.; Zeng, J.-H.; Yu, S.-H.; Yang, L.; Zhou, G.-E.; Qian, Y.-T. *Chem. Mater.* **2000**, *12*, 3259–3263.

of vancomycin and ATP released from the MSN material implied that ATP molecules were more strongly physisorbed to the organically functionalized mesoporous channels than the vancomycin molecules. On the basis of several reports in the literature,¹⁴ vancomycin has an isoelectric point (pI) of 8.3 and therefore is cationically charged under our experimental condition (pH 7.4). Conversely, ATP is anionic in pH 7.4 aqueous solutions. Given that the surface of the linker-MSN material is decorated with the 2-(propyldisulfanyl)ethylamine functionality, which is cationic (ammonium cation) at pH 7.4, the attractive electrostatic interaction between the ATP molecules and the linker-functionalized mesopores could be attributed to the stronger physisorption of ATP, whereas the repulsive electrostatic interaction between vancomycin molecules and the linker-derivatized mesopores disfavor the surface adsorption of vancomycin. These results suggested that perhaps only those molecules that are not in direct contact with the pore surface, i.e., nonphysisorbed molecules, could be released under our experimental conditions. Furthermore, in both vancomycin and ATP cases, the amount of drug release after 24 h of the addition of DTT showed similar DTT concentration dependencies (Figure 5b), indicating the rate of release is dictated by the rate of removing the CdS caps.

To demonstrate the biocompatibility and utility of our controlled-release delivery system for selective stimulation of certain cell types, ATP-loaded MSNs were introduced into an established astrocyte culture. It has been previously shown that ATP molecules evoke a receptor-mediated increase in intracellular calcium in astrocytes,¹⁵ which is an important regulatory mechanism for many intercellular communications and cooperative cell activities.¹⁶ Astrocyte type-1 cultures were obtained from neonatal rats by following previously published protocol¹⁷ to ensure the absence of neurons that complicate experimental interpretation. Phase-contrast microscopy indicated that cultures were indeed enriched in type-1 astrocytes and devoid of neurons. Immunocytochemistry experiments on these cells demonstrated that all the cultures are more than 95.0% immunopositive for glial fibrillary acidic protein (GFAP) and lacked MAP-2 immunoreactivity.¹⁸ The observed results further confirmed that these cultures are indeed type-1 astrocytes and not neurons. To determine the effect of ATP on cultured astrocytes, we used ratiometric-imaging techniques^{17,19} to monitor the glial calcium levels. Cells were loaded with the membrane-permeant Ca^{2+} -chelating fluorescent dye (Fura-2 AM),¹⁹ which is a widely used and highly sensitive indicator of intracellular calcium concentration ($[\text{Ca}^{2+}]_i$). The ATP-induced increases of $[\text{Ca}^{2+}]_i$ (calcium transients)¹⁹ represented by the color changes (increases of fluorescence) of the pseudocolor images of the cells were detected using an Attofluor system with Zeiss microscope.

To measure the effect of ATP released from the MSN system, astrocytes cultured in the presence of surface immobilized, CdS-capped MSNs with ATP molecules encapsulated inside of the mesoporous channels were first loaded with Fura-2 AM and then placed in a flow cell with a volume of 50.0 μL and a flow rate of 200.0 $\mu\text{L}/\text{min}$ in a flow direction from the top to the bottom of the images shown in Figure 6. As shown in Figure 6a and c, perfusion application of ME (1 mM for 5 min) resulted in a drastic decrease in the fluorescence intensity of CdS at the areas of the ATP-loaded MSN piles (MSN-1 and MSN-2) indicating the CdS caps have been released and diffused away from the surface-bound MSNs. Furthermore, we observed a pronounced increase in intracellular $[\text{Ca}^{2+}]_i$ represented by the color change of the pseudocolor images of Cell-1 and -2 (Figure 6a) and the corresponding upward shift of the red and blue curves of those two cells in the time course plot (Figure 6c). The observations suggested that the ATP molecules released from the mesoporous silica nanospheres located at the MSN-1 pile have reached their receptors on the cell surface of those astrocytes (for example, Cell-1 and -2) located at the downstream areas of the flow and thereby triggered the corresponding ATP receptor-mediated increase in intracellular calcium concentration. It is interesting to note that only the cells that were situated at the downstream areas relative to the MSN-1 pile (Figure 6a) are stimulated by the perfusion application of ME. Throughout the whole period of ME application, no obvious color changes could be observed in the pseudocolor images of those astrocytes that were located at the upstream areas, such as Cell-5, as shown in Figure 6a. The result indicated that the intracellular calcium concentrations of those "upstream" astrocytes relative to the MSN-1 pile were not affected by the perfusional introduction of ME. Given that the flow direction is from the top to the bottom of these images, such a phenomenon could be attributed to the fact that the ATP molecules released from the immobilized piles of MSNs by the perfusion application of ME could not diffuse against the flow to reach and stimulate the "upstream" astrocytes (Cell-5).

To confirm that the increase of $[\text{Ca}^{2+}]_i$ was not induced by the ME or the CdS released from the MSNs, two control experiments were performed. First, we obtained an enriched astrocyte type-1 culture via the same protocol but without the presence of MSNs. As shown in Figure 7, the perfusion application of ME (1.0 mM for 5 min) to these cells showed no increase in $[\text{Ca}^{2+}]_i$. A high concentration of ATP (100.0 μM) was later introduced to these ME-treated astrocytes. All cells responded to the ATP application with obvious increases in $[\text{Ca}^{2+}]_i$. Clearly, the ME application did not stimulate the calcium channel activity of these astrocytes to create any noticeable increase in $[\text{Ca}^{2+}]_i$. Also, such ME treatments did not cause any obvious damage to these cells and they could still respond normally to ATP stimulation.

To determine the effect of CdS nanoparticles on the $[\text{Ca}^{2+}]_i$ of astrocytes under our experimental conditions, we cultured the enriched type-1 astrocytes in the presence of CdS-capped MSNs without ATP encapsulation. Perfusion application of 100.0 μM ATP only increased the fluorescence intensity ($[\text{Ca}^{2+}]_i$ increased) of the areas where the astrocytes are located, whereas the fluorescence intensity of those of CdS-capped MSNs stayed constant as depicted in the pseudo-color images of the culture before (Figure 8a) and after (Figure 8b) the ATP application.

- (14) Takacs-Novak, K.; Noszal, B.; Tokes-Kovesdi, M.; Szasz, G. *Int. J. Pharm.* **1993**, *89*, 261–263 and references therein.
- (15) (a) Jeremic, A.; Jeftinija, K.; Stevanovic, J.; Glavaski, A.; Jeftinija, S. *J. Neurochem.* **2001**, *77*, 664–675. (b) Neary, J. T.; Laskey, R.; Van Breemen, C.; Blicharska, J.; Norenberg, L. O. B.; Norenberg, M. D. *Brain Res.* **1991**, *566*, 89–94. (c) Zhu, Y.; Kimelberg, H. K. *J. Neurochem.* **2001**, *77*, 530–541.
- (16) (a) Wang, Z.; Haydon, P. G.; Yeung, E. S. *Anal. Chem.* **2000**, *72*, 2001–2007. (b) Newman, E. A.; Zahs, K. R. *Science (Washington, D.C.)* **1997**, *275*, 844–847.
- (17) Jeftinija, S. D.; Jeftinija, K. V.; Stefanovic, G.; Liu, F. *J. Neurochem.* **1996**, *66*, 676–684.
- (18) See Supporting Information for the experimental details of immunocytochemistry and stimulatory effect of ATP on the cultured astrocytes.
- (19) Grynkiewicz, G.; Poenie, M.; Tsien, R. Y. *J. Biol. Chem.* **1985**, *260*, 3440–3450.

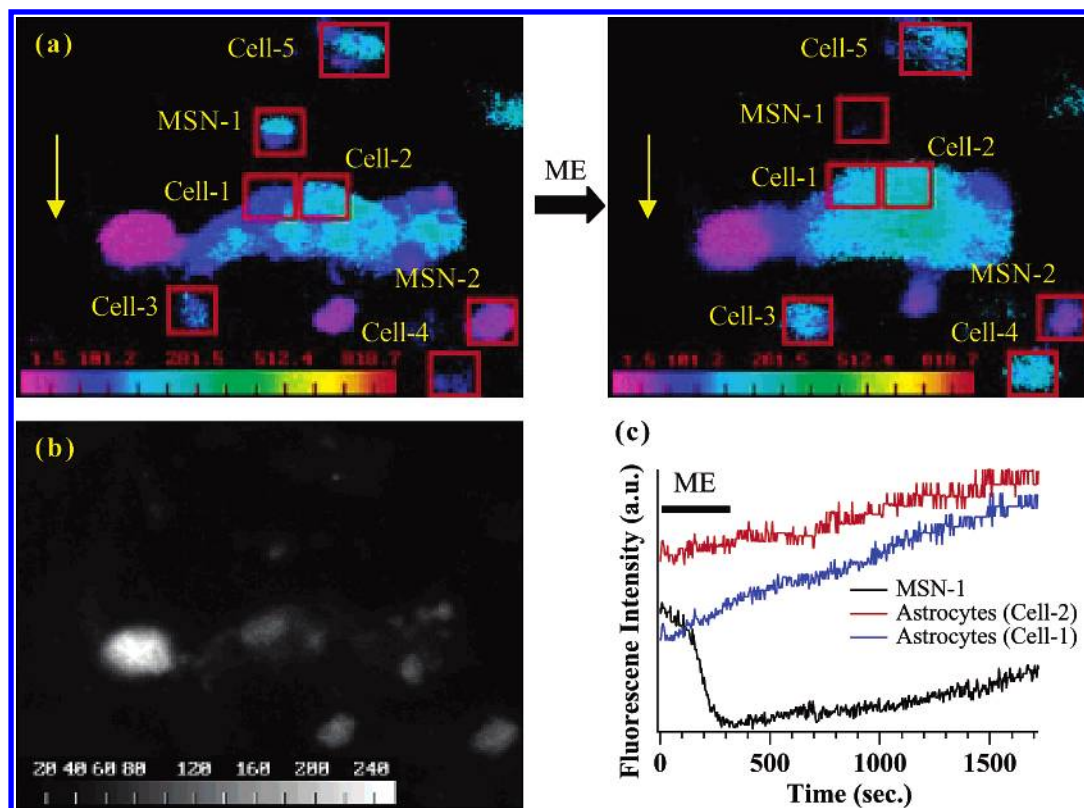


Figure 6. Effect of ATP release from CdS-capped MSNs on astrocytes. (a) Top panels show the pseudocolor images of astrocytes loaded with Fura-2 at resting level (top left panel) and after the application of ME (top right panel). The yellow arrows indicate the flow direction of HEPES buffer (pH 7.4). (b) Left bottom panel shows the fluorescence of cells and CdS at 520 nm ($\lambda_{\text{ex}} = 380$ nm). (c) Right bottom graph is a time course of astrocytes and CdS-capped MSN fluorescence prior to and after the application of ME. (Black bar represents the application time period of ME).

This result showed that apparently the astrocytes responded normally to ATP stimulation in the presence of CdS-capped MSNs. The culture of astrocytes and CdS-capped MSNs was then subjected to the same ME application. As shown in Figure 8b and c, no detectable changes in $[\text{Ca}^{2+}]_i$ were observed in the areas of astrocytes, but drastic decreases of fluorescence could be noticed easily in those areas of CdS-capped MSNs indicating the release of CdS caps upon ME application.

In conclusion, we have demonstrated that the organically functionalized MCM-41 type of mesoporous silica nanosphere material can be used as a novel controlled-release delivery carrier that are stimuli responsive. Given that the loading and release mechanism of the MSN system is based on the capping and uncapping of the openings of the mesopores with CdS nanoparticles, no chemical modification of the molecules of interest is needed. In addition, the biocompatibility and stability of the MSN material allow us to utilize such a system to investigate various intercellular chemical/neurochemical interactions in vitro. We envision that this MSN system could play a significant role in developing new generations of site-selective, controlled-release delivery, and interactive sensory nanodevices.

Experimental Section

Reagents and Materials. Cadmium nitrate tetrahydrate (99.99%), sodium sulfide, mercaptoacetic acid, 3-mercaptopropyltrimethoxysilane (MPTMS), *n*-cetyltrimethylammonium bromide (CTAB), tetraethyl orthosilicate (TEOS), 2-aminoethanethiol hydrochloride, 1-[3-(dimethylamino)propyl]-3-ethylcarbodiimide hydrochloride (EDC), dithiothreitol (DTT), and aldrithiol-2 were purchased (Aldrich) and used as received. Vancomycin hydrochloride and adenosine triphosphate disodium salt (ATP) were obtained from Sigma and used without further

purification. Nanopure water (18.1 MHz) prepared from a Barnstead E-pure water purification system was employed throughout. PBS buffer (10.00 mM, pH 7.4) solutions with the total ionic strength of 0.06 M were prepared and used as the solvent for all the loading and release experiments of vancomycin and ATP.

Synthesis of Mercaptoacetic Acid-Derivatized Cadmium Sulfide (CdS) Nanoparticles. The synthetic procedures were modified from the previous literature report by Alivisatos and co-workers.⁷ Mercaptoacetic acid (2.15×10^{-3} mol, 150.00 μL) was added to an aqueous solution (270.00 mL) of cadmium nitrate tetrahydrate (3.00×10^{-4} mol), forming a turbid blue solution, followed by adjusting the solution pH to 11 with 0.01 M NaOH. Sodium sulfide (1.50×10^{-4} mol) was dissolved in 10.0 mL of H_2O and rapidly added to the cadmium nitrate solution with vigorous stirring. The reaction mixture was protected from light and stirred for 10 min. It was concentrated to about one-tenth of its original volume using a rotary evaporator, and anhydrous methanol was added until the precipitate formed, yielding the mercaptoacetic acid-capped, water-soluble cadmium sulfide nanoparticles (CdS).

Synthesis of MCM-41-Type Mesoporous Silica Nanosphere with 2-(Propyldisulfanyl)ethylamine Functionality (Linker-MSN). The MSN material was synthesized by derivatization of a mercaptopropyl-functionalized mesoporous silica nanosphere material (thiol-MSN) prepared by the following procedures: *n*-Cetyltrimethylammonium bromide (CTAB, 1.00 g, 2.74×10^{-3} mol) was first dissolved in 480 mL of Nanopure water. NaOH(aq) (2.00 M, 3.50 mL) was added to CTAB solution, followed by adjusting the solution temperature to 353 K. TEOS (5.00 mL, 2.57×10^{-2} mol) was first introduced dropwise to the surfactant solution, followed by the dropwise addition of MPTMS (0.97 mL, 5.13×10^{-3} mol). The mixture was allowed to stir for 2 h to give rise to white precipitates (as synthesized thiol-Sphere). The solid product was filtered, washed with deionized water and methanol, and dried in air. To remove the surfactant template (CTAB), 1.50 g of as-synthesized thiol-Sphere was refluxed for 24 h in a solution of 9.00

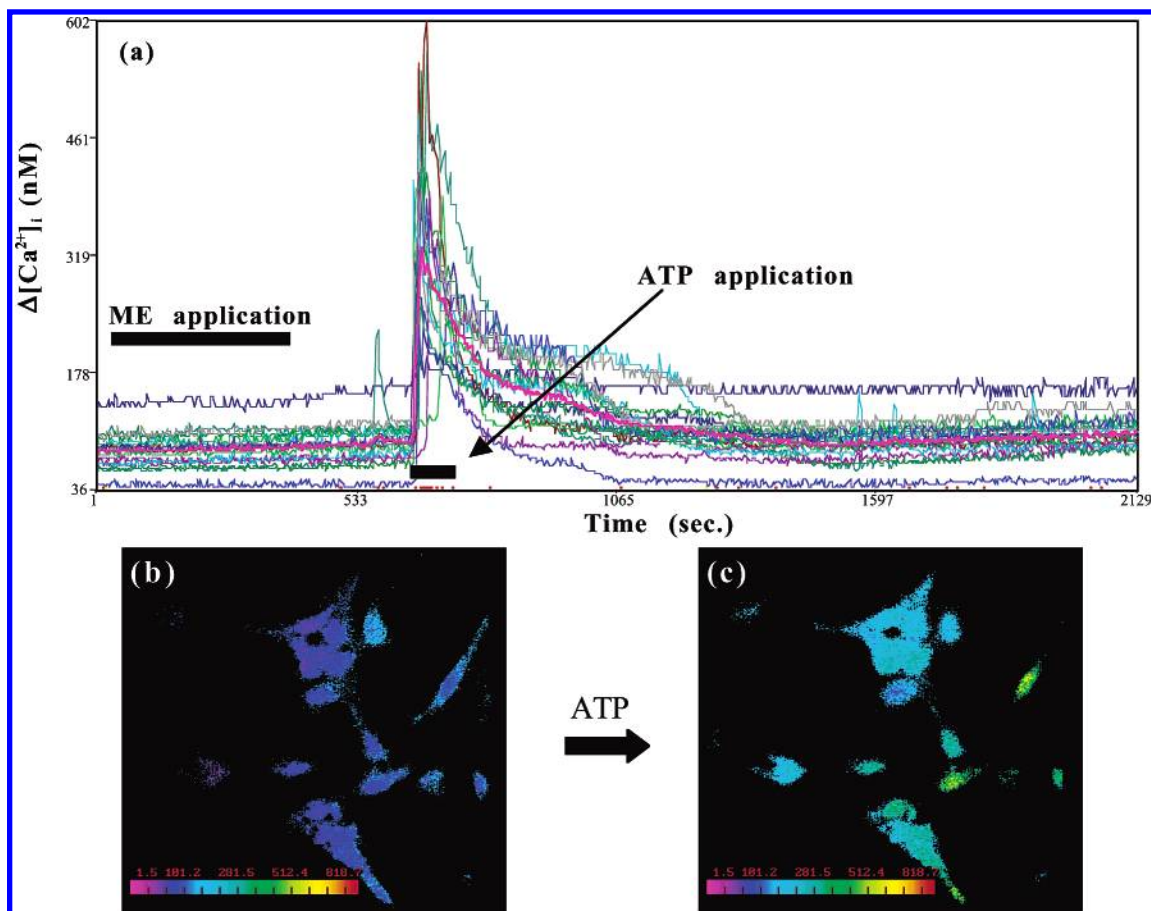


Figure 7. (a) Images showing that application of ME on an astrocyte culture loaded with the intracellular Ca^{2+} -chelating fluorophore (Fura 2-AM) without the presence of MSN failed to produce any $[\text{Ca}^{2+}]_i$ response of astrocytes. (b) Pseudo-color image of astrocytes taken after the ME application showed no increase or decrease in $[\text{Ca}^{2+}]_i$ of the cells. (c) The same cells responded to the perfusion application of 100.0 μM ATP indicated by the increase of fluorescence intensity of the pseudo-color image of astrocytes, i.e., $[\text{Ca}^{2+}]_i$ increases.

mL of HCl (37.4%) and 160.00 mL of methanol followed by extensive washes with deionized water and methanol. The resulting surfactant-removed thiol-MSN material was placed under high vacuum to remove the remaining solvent in the mesopores. The chemically accessible thiol group surface coverage of the thiol-MSN material was quantified to be 7.64×10^{-4} mol/g by our previously published method.^{9a} The purified thiol-MSN material (1.00 g) was treated with a methanol solution (60.00 mL) of 2-(pyridyldisulfanyl)ethylamine (PDEA) (9.12×10^{-4} mol), which was synthesized via a literature procedure,¹⁰ at room temperature for 24 h under vigorous stirring to undergo the desired disulfide bond exchange reaction. The resulting MSN material with 2-(propyldisulfanyl)ethylamine functionality was filtered and washed with methanol and dried in air.

Loading of Vancomycin and ATP into the Mesoporous Framework of Linker-MSN and the Capping of the Mesopores with Mercaptoacetic Acid-Functionalized CdS Nanoparticles. The purified linker-MSN material (100.00 mg) was incubated in the aforementioned PBS buffer solution (0.60 mL, pH 7.4) of ATP or vancomycin (3.00 μmol in both cases) for 24 h. The mercaptoacetic acid-functionalized CdS nanoparticles (0.15 mmol) were dissolved in 2.00 mL of PBS buffer with vancomycin or ATP (0.01 mmol in both cases). 1-[3-(Dimethylamino)propyl]-3-ethylcarbodiimide hydrochloride (EDC) (57.50 mg, 0.30 mmol) was added to the CdS/drug solution. The reaction mixture was allowed to stir for 24 h, followed by centrifuging the suspension at 12 000 rpm for 3 min. The resulting precipitates (ATP- or vancomycin-loaded, CdS-capped MSNs) were isolated and dried under vacuum.

DTT-Induced Drug/Neurotransmitter Release Study. CdS-capped MSN with vancomycin or ATP (10.00 mg) material was dispersed in

1.50 mL of PBS buffer (pH 7.4), followed by repeating wash/sonication/centrifugation cycles for five times to remove physisorbed, uncapped vancomycin or ATP molecules on the exterior surface of the material. The purified MSN/drug composite was redispersed in 3.50 mL of PBS buffer (pH 7.4). Aliquots were taken every 4 h over a time period of 12 h from the MSN/water suspension and injected to an analytical HPLC system (Hitachi LC/3DQMS with a reverse phase C18 column (Vydac), 0.4 cm \times 25 cm) to monitor the leaching of the mesoporous channel encapsulated vancomycin or ATP molecules. After 12 h, dithiothreitol (DTT, 18.50 mM) was added to the suspension to cleave the disulfide linkage between the CdS nanoparticle and the MSN. The kinetic profiles of the DTT-induced release of vancomycin and ATP were monitored by following two literature-reported HPLC separation conditions.²⁰ The peaks/areas at 280 and 258 nm were monitored/integrated for the quantitative analysis of amounts of released vancomycin and ATP, respectively.

Instrumental Methods, Conditions, and Parameters for the Structure Characterizations of Linker-MSN and CdS-Capped MSN Materials. Powder XRD diffraction data were collected on a Scintag XRD 2000 X-ray diffractometer using Cu K α radiation. Nitrogen adsorption and desorption isotherm, surface area (SA), and median pore diameter (MPD) were measured using a Micromeritics ASAP2000 sorptometer. Sample preparation included degassing at 130 $^{\circ}\text{C}$ for 1 h. Nitrogen adsorption and desorption isotherms of these materials were obtained at -196 $^{\circ}\text{C}$. Specific surface areas and pore size distributions were calculated using the Brunauer–Emmett–Teller (BET) and Bar-

(20) (a) Farin, D.; Piva, G. A.; Gozlan, I.; Kitzes-Cohen, R. *J. Pharm. Biomed. Anal.* **1998**, *18*, 367–372. (b) Veciana-Nogues, M. T.; Izquierdo-Pulido, M.; Vidal-Carou, M. C. *Food Chem.* **1997**, *59*, 467–472.

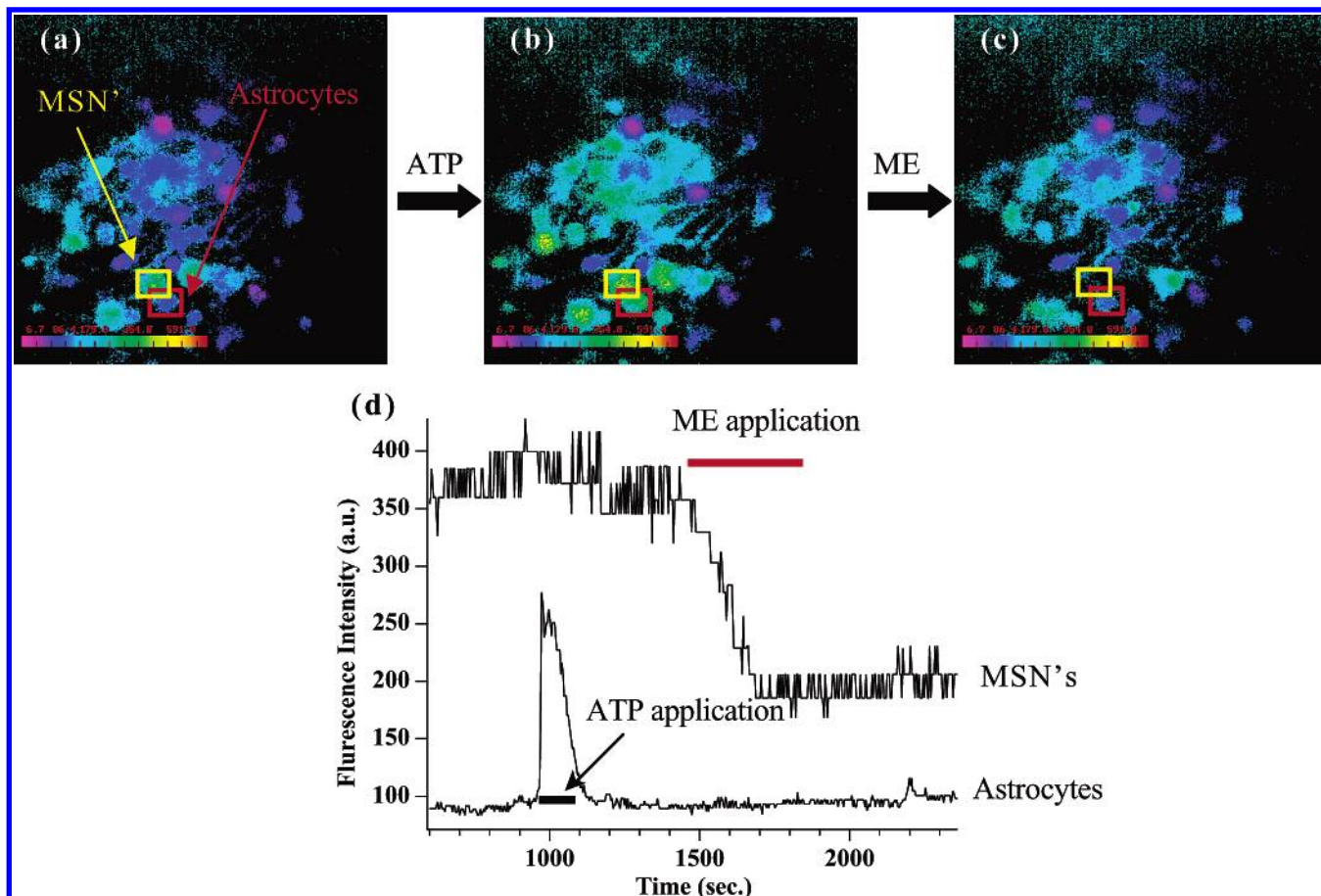


Figure 8. Pseudo-color images of an astrocyte culture in the presence of random piles of CdS-capped MSNs with empty mesoporous channels (no ATP encapsulation) before (a) and after (b) the application of ATP (100.0 μ M). An increase in $[Ca^{2+}]_i$ of the astrocytes (lower square, red) located adjacent to a pile of MSNs (upper square, yellow) upon the perfusion application of ATP was observed (d, lower curve). The result suggested that the astrocytes are responsive to ATP stimulation. Interestingly, significant decrease of the fluorescence intensity (c and d, upper curve) of the pile of MSNs (upper square, yellow) was observed upon the perfusion application of ME due to the uncapping of CdS (diffusing away from the area of interest). Concurrently, the adjacent astrocytes did not show any detectable response during the application of ME.

rett–Joyner–Halenda (BJH) method, respectively. Particle morphology of these materials was determined by scanning electron microscopy (SEM) using a JEOL 840A scanning electron microscope with 10 kV accelerating voltage and 0.005 nA of beam current for imaging. For transmission electron microscopy (TEM) studies, a small aliquot was removed and placed between two clean glass slides. Slides were squeezed between fingers and rubbed back and forth to break up larger clumps. The resulting powder was washed into a Petri dish with acetone. The mixture was stirred and ultrasonically agitated. While still in suspension a lacey carbon-coated TEM grid was pulled through the suspension. The grid was allowed to dry in air and then examined in an Amray 1845 FE-SEM followed by examination with a Philips model CM-30 TEM operated at 300 kV. The specimen was given no further treatment, as it appeared stable under beam bombardment. The preparation for the microtomed samples included embedding into a derivation of EPON epoxy resin using EmBed 812. This mixture was centrifuged and cured for 24 h at 60 $^{\circ}$ C. The embedded block was microtomed to obtain thin sections of 60–80-nm thickness by using a Reichert Ultracut S ultramicrotome with a diamond knife (Diatome). The floated sections were mounted on a 400 mesh Pd-coated Cu grid. The TEM images of these microtomed samples were recorded using a Philips model CM-30 TEM operated at 300 kV at 69 000 to 340 000 electron optical magnification.

Experimental Methods and Conditions for Controlled-Release Studies of CdS-Capped, ATP-Encapsulated MSN with Neuroglia Cells (Astrocytes) in Vitro. **Methods.** Wistar rats, raised at Iowa State University, were used for these experiments. Animal care and experi-

mental protocols were in accordance with the guidelines and approval of the Iowa State University Committee on Animal Care.

Cell Cultures. Enriched primary astrocyte cultures from neonatal (P_0 to P_3) rat cerebral cortex were prepared as previously described.^{15a} Briefly, freshly dissected cortical tissues from three animals were incubated 50 min at 37 $^{\circ}$ C in 2.00 mL of Earle's balanced salt solution (EBSS; Gibco-Invitrogen Co.) containing papain (1.54 mg/mL; Sigma-Aldrich Co.). After incubation, tissue was rinsed with EBSS solution and incubated for 5 min in trypsin-inhibitor solution (1 mg/mL; Gibco-Invitrogen Co.). After being rinsed, once with EBSS solution and once with culture medium (consisting of α -minimum essential medium (α -MEM; Gibco-Invitrogen Co.) supplemented with 10% heat-inactivated fetal bovine serum (FBS; Gibco-Invitrogen Co.) and 1.00 mL of penicillin–streptomycin solution (Sigma-Aldrich Co.) per 100 mL), the tissue was mechanically dispersed in culture medium by triturating through a fire-polished glass pipet. The cell suspension was transferred to sterile 15-mL centrifuge tubes and spun at 1000g for 10 min. Cell pellets were resuspended in culture medium (α -MEM supplemented with 10% heat-inactivated FBS and 1.00 mL of penicillin–streptomycin solution per 100.00 mL) and plated in culture flasks. Cells were maintained at 37 $^{\circ}$ C in a humidified 5% CO_2 /95% air atmosphere. Culture medium was changed every 2 to 3 days. When mixed cultures reached confluence (9–12 days), the flasks were shaken (260 rpm) for 90 min to remove microglia and dividing type I astroglia. After shaking the cells, medium was replaced, and the flasks were incubated for 1 h to equilibrate with CO_2 in the fresh medium. Cultures were then shaken overnight (12–18 h) at 260 rpm at 37 $^{\circ}$ C. Cultures enriched in type I

astroglia were obtained by trypsinizing (0.25%; Sigma-Aldrich Co.) attached cells for 5 min. Trypsin was inactivated by adding α -MEM supplemented with the 10% heat-inactivated FBS (serum contains protease inhibitors). Cells were plated on poly-L-lysine-coated coverslips (10.00 μ g/mL; MW 100 000; Sigma-Aldrich Co.) at a density of 3.00×10^4 cells/cm². All experiments were performed on cells that had been in culture for 2–4 days after replating.

Characterization of Glial Cultures. An antibody against glial fibrillary acidic protein (GFAP) was used to identify astrocytes following the procedure described in the subsequent Immunocytochemistry section. We confirmed that glial cultures were neuron-free by using antibodies against the tubular protein MAP-2. In astrocyte-enriched cultures immunoreactivity for MAP-2 was absent, while neurons were immunopositive in parallel cultures that contained neurons.

Immunocytochemistry. After fixation with 4% paraformaldehyde (Fisher Chemical) for 30 min at room temperature, cells were incubated for 30 min in a 50% goat serum solution containing 1% bovine serum albumin (BSA; Sigma-Aldrich Co.) and 100.00 mM L-lysine (Sigma-Aldrich Co.), to block nonspecific binding, and 0.4% Triton X-100 to permeabilize the membrane. Immunocytochemistry was performed using antibodies raised against glial fibrillary acidic protein (GFAP; 1:5000; Sigma-Aldrich Co.) and microtubule associated protein (MAP-2; 1:2000; Sigma-Aldrich Co.). Positive controls were established with these antibodies using cortical glia and neurons. Negative controls were established by omitting the specific antiserum. Antibody visualization was accomplished by the employment of the biotinylated secondary antibody, the Vectastain ABC kit (Vector) and the nickel-enhanced 3-3'-diaminobenzidine method.²¹ Cells were dehydrated in graded alcohol, cleaned in xylene, and sealed with acrytol on glass slides.

Intracellular Calcium Imaging. The effect of experimental manipulation on the intracellular calcium concentration ($[Ca^{2+}]_i$) of cultured

cells was evaluated by ratiometric imaging techniques.¹⁷ Cells were loaded with Fura 2-AM (5.00 μ M; Molecular Probes) for 40–60 min at 37 °C; 1.00 μ L of 25% (w/w) of Pluronic F-127 (Molecular Probes) was mixed with every 4.00 nM of AM ester to aid solubilization of the ester into aqueous medium. Coverslips containing glial cells were washed with normal Hepes–saline solution and further incubated for 10 min at 37 °C to allowed de-esterification of Fura 2-AM. Normal Hepes–saline solution contains (in mM): NaCl 140.00, KCl 5.00, MgCl₂ 2.00, CaCl₂ 2.00, and HEPES (Sigma-Aldrich Co.) 10 (pH 7.4). All image processing and analysis were performed using an Attolfluor system with Zeiss microscope. Background subtracted, rationed images (340/380 nm) were used to calculate the $[Ca^{2+}]_i$ according to a literature-reported method.¹⁹ Calibration was performed in situ according to the procedure provided by the Attolfluor, using the Fura-2 Penta K⁺ salt (Molecular Probes) as a standard. Using wavelengths of 340 and 380 nm, Fura 2-AM was excited, and the emitted light was collected at 520 nm.

Acknowledgment. This research was supported by the United States DOE Ames Laboratory (MPC-PSI grant) and the NSF (CAREER award: CHE-0239570 and IBN-9604862). We thank Dr. M. J. Kramer and Mr. F. C. Laabs for experimental assistance in TEM measurements of the materials and helpful discussions.

Supporting Information Available: Spectroscopic characterizations of the organically functionalized MSN and the CdS-capped MSN; experimental details of immunocytochemistry on astrocyte cultures (PDF). This material is available free of charge via the Internet at <http://pubs.acs.org>.

(21) Jeftinija, S.; Liu, F.; Jeftinija, K.; Urban, L. *Regul. Pept.* **1992**, *39*, 123–135.